

# Kubelka-Munk Theory and the MTF of Paper

J. S. Arney,<sup>▲</sup> Jim Chauvin,<sup>▲</sup> Josh Nauman, and Peter G. Anderson<sup>▲</sup>

Center for Imaging Science, Rochester Institute of Technology, Rochester, New York, USA

An experimental analysis of paper optical scattering is reported. The Kubelka–Munk parameters for scattering,  $S$ , absorption,  $K$ , thickness,  $L$ , and background reflectance,  $R_g$ , were measured for a variety of papers. Measurements were made of reflectance and transmittance using integrating sphere techniques, and the Kubelka–Munk Eqs. were inverted numerically to generate the corresponding  $S$  and  $K$  values. The modulation transfer function, MTF, of each paper sample was also measured by projecting a sharp edge onto the paper and measuring the resulting edge spread function. The MTF was calculated as the modulus of the Fourier transform of the derivative of the edge function. The inverse of the frequency at which the MTF = 0.5 was used as an index of the MTF and called  $k_p$ . Values of  $k_p$  were compared to values of the Kubelka–Munk parameters. Through a combination of theory and empirical observation, a model was developed to relate  $k_p$  to  $S$ ,  $K$ , and  $L$  for  $R_g = 0$ . The results strongly indicate that an additional parameter is required in order to rationalize the observed MTF of papers. This additional parameter is suggested to be the scattering homogeneity of the paper.

Journal of Imaging Science and Technology 47: 339–345 (2003)

## Introduction

The objective of this project was to explore experimentally the relationship between two well known ways of describing light scattering in paper. One, the Kubelka–Munk theory, has been used extensively and quite successfully in the literature to describe reflectance and opacity of paper and of images printed on paper.<sup>1–4</sup> The other is the MTF function, which describes lateral light scattering in paper and is used to describe color and tone reproduction in printed halftone images.<sup>5–7</sup> Intuitively, these two descriptions of describing light scattering should be related, and experiments have been reported that demonstrate a correlation between the two.<sup>8–10</sup> The current report describes an experimental study of the relationship between paper MTF and Kubelka–Munk theory. As will be shown, Kubelka–Munk theory provides most, but not all, of the parameters needed to describe the MTF characteristics observed for many common types of paper.

## Background

The phenomenon called the Yule–Nielsen effect is based on the use of Eq. (1) to predict the reflectance,  $R$ , of a halftone image.<sup>11,12</sup>

$$R = F \cdot R_k + (1 - F) \cdot R_p \quad (1)$$

$F$  is the dot area fraction on the paper,  $R_k$  is the reflectance of a solid patch of ink printed at  $F = 1$ , and  $R_p$  is the reflectance of the unprinted paper. The reflectance predicted by Eq. (1) is generally higher than the measured reflectance. The fundamental cause of optical dot gain is well known to be the lateral scattering of light within paper.<sup>13</sup> Light that enters the paper between the halftone dots can scatter laterally within the bulk of the paper before returning to the surface as reflected light. This lateral scattering in the bulk of the paper increases the probability the light will encounter a halftone dot and be absorbed. Thus the effective absorption cross section of the halftone dot is larger than the physical size of the dot, so the term “optical dot gain” is often used.

The expected reflectance of a halftone image may also be estimated with Eqs. (2) and (3), where  $T(x,y)$  is the transmittance pattern of the ink on the paper and  $A$  is the area of the paper over which the average reflectance is measured.<sup>2,14</sup>  $PSF(x,y)$  is a probability density function that describes the probability of a photon returning to the surface of the paper at a location  $(x,y)$  away from the point of entry into the paper. The operator  $*$  in Eq. (2) is the convolution operator, and convolution is commonly carried out by multiplying the Fourier transforms of  $T$  and  $PSF$  and then taking the inverse transform, as shown in Eqs. (4) and (5). The Fourier transform of the point spread function,  $FFT\{PSF\}$ , is called the modulation transfer function, MTF, of the paper, and the lateral scattering characteristic of the paper is often described by either the  $PSF$  function or the MTF function.

$$R(x,y) = R_p \cdot T(x,y) \cdot [T(x,y) * PSF(x,y)] \quad (2)$$

$$R = \frac{1}{A} \cdot \iint_{x,y} R(x,y) dx dy \quad (3)$$

Original manuscript received December 18, 2002

▲ IS&T Member

©2003, IS&T—The Society for Imaging Science and Technology

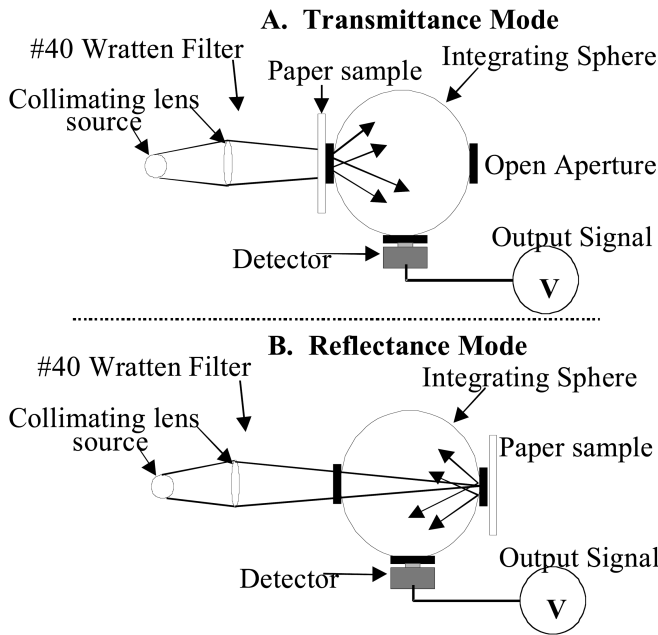


**Figure 1.** Integrating sphere instrument assembled to measure (A) transmittance and (B) reflectance. The #40 Wratten filter confined the measurements to the green region of the spectrum.

$$T(x,y)*PSF(x,y) = iFFT\{ FFT\{T(x,y)\} \cdot FFT\{PSF(x,y)\} \} \quad (4)$$

$$MTF(\omega,\nu) = FFT\{PSF(x,y)\} \quad (5)$$

The Kubelka–Munk theory describes the reflectance and opacity properties of materials in terms of four parameters; the thickness of the material,  $z$ , the reflectance;  $R_g$ , of whatever is behind the material; an absorption coefficient,  $K$ ; and a scattering coefficient,  $S$ . The absorption and scattering coefficients are expressed in units of inverse distance,  $\text{mm}^{-1}$ , and are inversely proportional to the mean distance that a photon travels in the material before it is absorbed,  $K$ , or scattered,  $S$ .

Kubelka–Munk theory is expressed in terms of differential equations.<sup>15</sup> Equations (6) and (7) are general solutions of the Kubelka–Munk theory for the transmittance,  $T$ , and reflectance,  $R$ , of paper. Both  $R$  and  $T$  can be measured with an integrating sphere instrument, as illustrated in Fig. 1. Equations (6) and (7) are invertible, so measured values of  $R$ ,  $T$ ,  $R_g$ , and  $z$ , were used in the current project to determine experimental values of  $S$  and  $K$ . These Kubelka–Munk parameters were then compared to values of MTF measured for a wide range of paper types.

$$T = \frac{b}{a \cdot \text{Sinh}(b \cdot S \cdot z) + b \cdot \text{Cosh}(b \cdot S \cdot z)} \quad (6)$$

where  $a = \frac{K}{S} + 1$  and  $b = \sqrt{b^2 - 1}$

$$R = \frac{1 - R_g \cdot (a - b \cdot \text{Coth}(b \cdot S \cdot z))}{a - R_b + b \cdot \text{Coth}(b \cdot S \cdot z)} \quad (7)$$

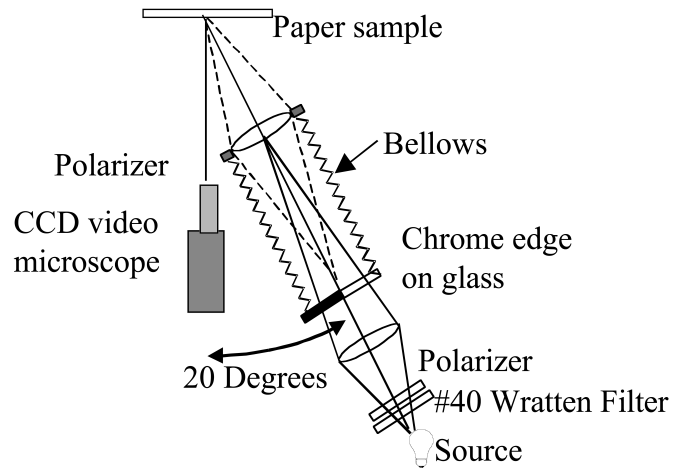


**Figure 2.** Projected edge technique for measuring paper MTF.

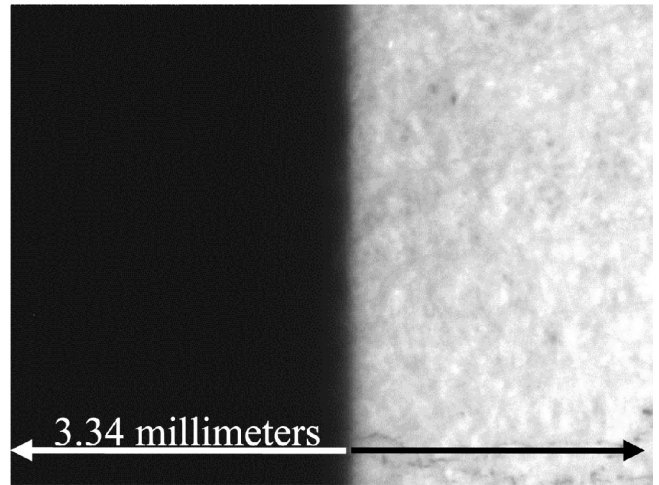


**Figure 3.** Image of the edge projected onto a thick stack of office copy paper (20 lb basis weight)

### Measurement of Paper MTF

The most common and practical manifestation of paper MTF is the phenomenon of optical dot gain. However, more direct measure of the MTF can be done by the analytical procedure described by Yule and others<sup>10–12</sup> and illustrated in Fig. 2. An edge of light is focused onto the paper sample, and the bulk reflected light is measured. The instrument shown in Fig. 2 for the current project included the same green filter used in the integrating sphere measurements. In addition, crossed polarizers were used to eliminate first surface reflections from the measurement. Figure 3 illustrates an edge image captured with this system for an ordinary office copy type of paper.

The camera used to capture edge images produced pixel values linearly related to radiance of the object. The edge trace was generated by calculating the mean pixel value in each vertical row. The mean values were plotted versus the horizontal dimension, as shown in Fig. 4. The derivative of this edge function, called the line spread function LSF, was estimated as the point by point difference between consecutive values in the edge trace. This also is illustrated in Fig. 4.

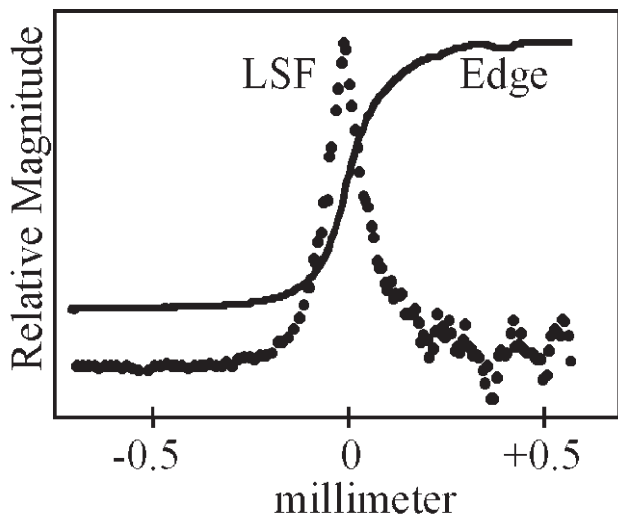


**Figure 4.** Edge trace and line spread function, LSF, for the image in Fig. 3.

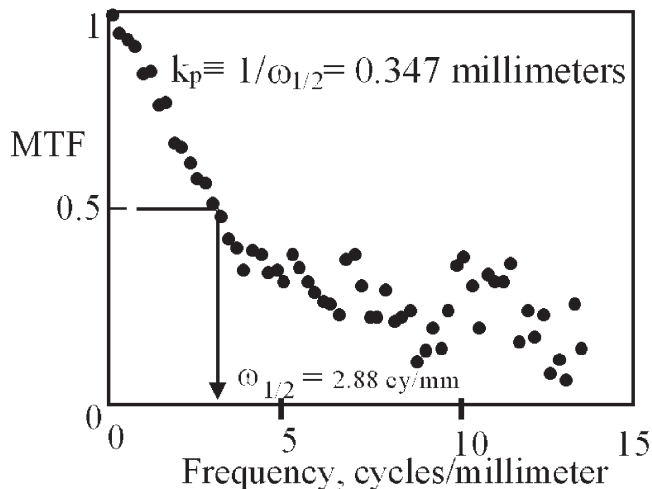


**Figure 5.** Modulus of the Fourier Transform of the LSF data in Fig. 4, normalized to 1 at the origin.

The one dimensional MTF( $\omega$ ) is the Fourier transform of the line spread function, LSF( $x$ ). A fast Fourier transform algorithm applied to the LSF data in Fig. 4 produced the experimental estimate of the paper MTF shown in Fig. 5.

In order to compare MTF curves to Kubelka–Munk parameters for a wide range of paper samples, a single metric was selected to represent the MTF. This metric is the inverse of the frequency at which the MTF = 0.5. As illustrated in Fig. 5, the value is  $k_p = 0.347$  for the paper sample in this illustration. Table I shows the experimental data collected for the paper samples in this study. MTF measurements were made for single sheets with black backing (finite  $k_p$ ) and for sheets stacked to infinite thickness (infinite  $k_p$ ). Values of  $S$  and  $K$  were measured for single sheets with no backing, which is close to a perfect black backing,  $R_g = 0$ . Figure 6 summarizes the correlation between the MTF parameter,  $k_p$ , and the scattering coefficient,  $S$ .

#### The Parameters Governing $k_p$

Figure 6 clearly confirms the expected correlation between the Kubelka–Munk scattering coefficient and the MTF of paper at infinite thickness. The correlation for samples at finite thickness is very poor, but the general impact of thickness is clearly demonstrated. Thin sheets have smaller  $k_p$  values, which means their MTF is better. This makes sense because MTF is degraded when light is able to travel laterally in the paper, but if the sheet is thin, light passes through and does not have as much opportunity to undergo lateral scattering.

The impact of the absorption coefficient,  $K$ , on  $k_p$  has been explored previously,<sup>16</sup> and for values of  $K < 5 \text{ mm}^{-1}$ , no effect was reported on the value of  $k_p$ . This is consistent with the observation in Table I that samples 5 and 6 have the same  $S$  and  $k_p$  values when stacked to infinity even though they have significantly different  $K$  values. Thus, the experimental evidence indicates that the MTF of common papers is significantly influenced by thickness and  $S$  but insignificantly influenced by  $K$ .

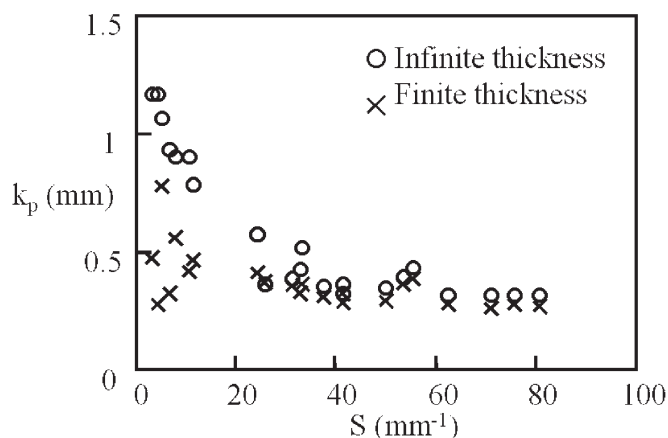


**Figure 6.** Experimental values of  $k_p$  versus experimental values of  $S$  for paper samples at both infinite thickness,  $O$ , and finite thickness,  $X$ .

#### The Oittinen–Engeldrum Model

The relationship between Kubelka–Munk theory and the MTF of paper suggested by Oittinen<sup>8,9</sup> and by Engeldrum<sup>10</sup> is illustrated in Fig. 7. Diagram (A) illustrates the increase in reflectance of paper,  $R_R(z)$ , as the thickness,  $z$ , of the paper increases. This relationship is described by Eq. (7) in Kubelka–Munk theory with  $R_g = 0$ . Diagram (B) illustrates the change in reflectance,  $R_p(r)$ , as a function of distance,  $r$ , from the point of entry of the light into the paper. The Oittinen assumption is that the curve in (B), which is the point spread function, is the same as the derivative of the curve in (A).

Engeldrum suggested a quantitative derivation of the paper MTF by taking the derivative of the Kubelka–Munk function for reflectance and then taking the Hankel transform.<sup>10</sup> With some simplifying assumptions, Engeldrum derived Eq. (8) for the MTF of paper, where  $R_\infty = a - b$ .

**TABLE I. Summary of Experimental Data**

Tr = tracing paper P = plastic non fiber sheet, NC = non-coated paper, News = newsprint, SC = super-calandared, C = coated. Thickness, and  $k_p$  are in millimeters. S and K are in  $\text{mm}^{-1}$ .

Sample	Type	Thickness	S	K	Finite $k_p$	Infinite $k_p$
1	Tr	0.042	4.24	0.22	0.274	1.167
2	Tr	0.071	10.13	0	0.42	0.9
3	Tr	0.0455	4.93	0	0.78	1.067
4	Tr	0.0765	11.18	0	0.466	0.783
5	NC	0.097	41.17	0.51	0.326	0.363
6	News	0.1095	41.2	2.48	0.282	0.327
8	NC, SC	0.095	80.25	0.58	0.267	0.32
9	NC	0.098	31.03	0	0.357	0.383
10	Tr, P	0.089	6.5	0	0.323	0.933
11	Tr	0.13	2.92	0	0.473	1.167
12	NC, SC	0.084	23.84	0	0.414	0.573
13	NC	0.065	62.17	0.65	0.274	0.313
14	C	0.089	70.67	0.84	0.264	0.317
15	NC	0.122	25.33	0	0.372	0.367
16	NC	0.126	37.27	0.28	0.312	0.353
17	NC	0.099	32.83	0.18	0.364	0.523
18	NC	0.124	49.66	0.24	0.294	0.347
19	NC	0.104	32.4	0	0.328	0.423
20	Tr, P	0.11	7.52	0	0.56	0.990
21	NC, SC	0.293	53.01	0.49	0.366	0.397
22	C	0.093	75.17	0.54	0.28	0.32
23	NC, SC	0.13	55.25	0.48	0.387	0.433

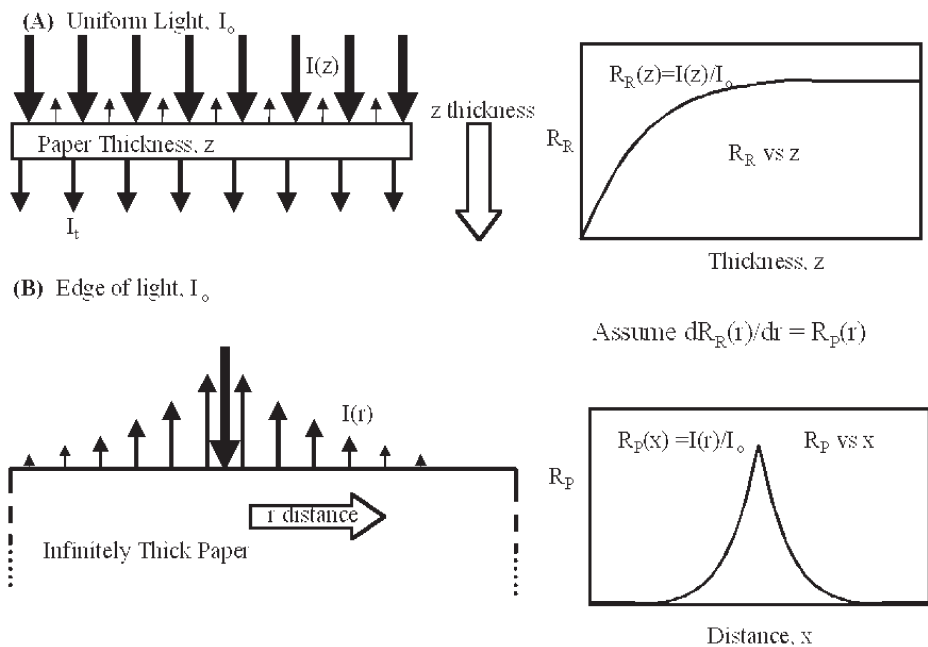


**Figure 7.** Schematic Interpretation of Oittinen-Engeldrum Model

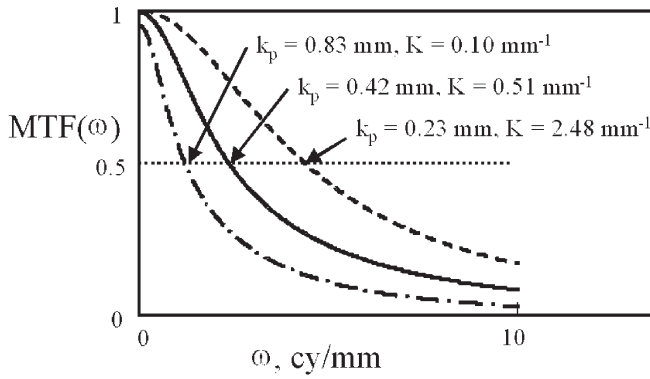


**Figure 8.** MTF curves calculated with Eq. (8) for  $S = 41 \text{ mm}^{-1}$  and values of  $K$  shown. Compare with Table I, samples 5 and 6.

$$\text{MTF}(\omega) = \frac{1}{\ln\left[\frac{1}{1-R_\infty^2}\right]} \cdot \sum_{j=1}^{\infty} \frac{R_\infty^{2j}}{j} \cdot \left[1 + \left(2\pi \frac{\omega}{2bSj}\right)^2\right]^{-3/2} \quad (8)$$

Equation (8) is plotted in Fig. 8 for  $S = 41 \text{ mm}^{-1}$  for three different values of  $K$ . Two of the calculations represent samples 5 and 6 in Table I. The values of  $K = 0.10$  and  $0.51$  represent an absorption event about once every 10 mm and 2 mm, respectively. Thus, they are essentially zero relative to the typical scattering distances in papers, but the values of  $k_p$  are predicted to be quite different. It is evident, as suggested previously, that Eq. (8) over estimates the involvement of  $K$  in the MTF of paper.

#### An MTF Model With $K = 0$

By far the majority of paper samples used to print half-tone images have low absorption coefficients, so it seems reasonable to alter the derivation suggested by Engeldrum by starting with the Kubelka–Munk solution for  $R$  with  $K = R_g = 0$ . Equation (9) is such a solution.

$$R = \frac{S \cdot z}{S \cdot z + 1} \quad (9)$$

As suggested by Oittinen and by Engeldrum, we estimate the point spread function as the derivative of Eq. (9), substituting thickness,  $z$ , with lateral distance,  $r$ . This leads to Eq. (10).

$$\text{PSF}(r) = \frac{S}{(S \cdot r + 1)^2} \quad (10)$$

The inverse of the scattering coefficient is a distance,  $L = 1/S$ , that is proportional to the mean distance light travels between encounters with a scattering center. We define a normalized distance,  $\ell = S \cdot r$ . This is distance in units of scattering distance,  $L$ . In units of  $L$ , the scattering coefficient is always unity, so the normalized point spread function for any scattering coefficient becomes Eq. (11).

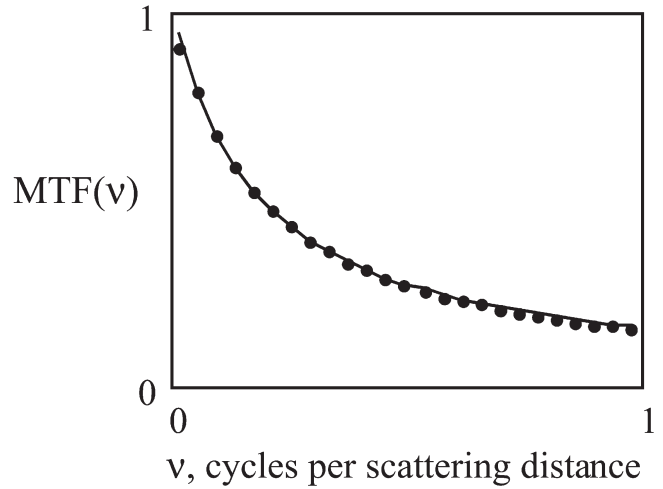


**Figure 9.** The  $\text{MTF}(v)$  of paper at infinite thickness with frequency expressed in cycles per scattering length.

$$\text{PSF}(\ell) = \frac{1}{(\ell + 1)^2} \quad (11)$$

The one dimensional  $\text{MTF}(v)$  function is the Hankel transform of the PSF, where  $J_0$  is the first order Bessel function, with frequency,  $v$ , expressed in cycles per scattering length ( $\text{cy}/\ell$ ).

$$\text{MTF}(\omega) = \int_0^{\infty} \text{PSF}(\ell) \cdot J_0(2\pi\omega\ell) d\ell \quad (12)$$

Numerically, Eq. (13) is a close approximation of Eq. (12). Both Eqs. are plotted in Fig. 9, where the dots are Eq. (12) and the line is Eq. (13).

$$\text{MTF}(v) = \frac{1}{1 + 5.4v} \quad (13)$$

The frequency  $v$  in  $\text{cy}/\ell$  is related to the frequency  $\omega$  in  $\text{cy}/\text{mm}$  as follows.

$$v = \omega/S \quad (14)$$

The value of  $k_p$  is the value of  $\omega$  for  $\text{MTF} = 1/2$ , so Eqs. (13) and (14) lead to Eq. (15) as a model for  $k_p$  at infinite thickness. The dotted line in Fig. 10 shows Eq. (15) plotted with the experimental data for  $k_p$  measured at infinite thickness. This simple model seems to capture the general shape of the relationship between  $k_p$  and  $S$ , but the model significantly undershoots the experimental data.

$$k_p = 5.4/S \quad (15)$$

#### Empirical Modifications of the MTF Model

The disagreement between Eq. (15) and the experimental data at first glance might seem to reflect an

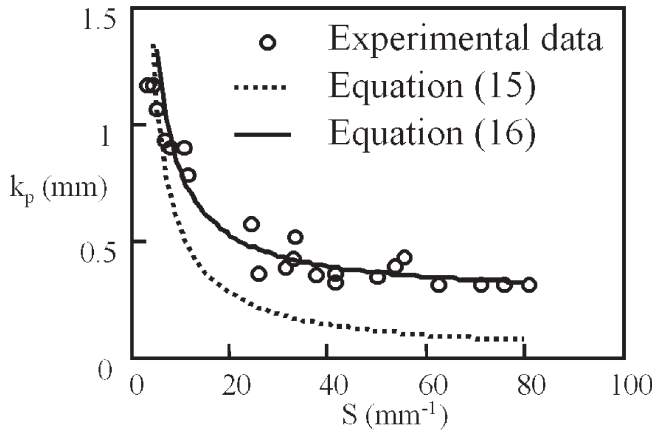


**Figure 10.** Modeled and measured  $k_p$  versus  $S$  for in finitely thick samples.

experimental error of neglecting the MTF characteristics of the instrument used to measure the paper samples. However, separate measurements of the chrome edge placed at the paper sample location in Fig. 2, illuminated diffusely from the rear, provided an estimate of the instrument MTF. The result was  $\text{MTF} = 1/2$  at 40 cycles/mm, and correction for the instrument MTF made no significant difference to the experimental data. There is always the potential for unanticipated experimental artifacts, but if the data in Fig. 10 are reasonably accurate, it appears the MTF of paper asymptotically approaches a value of  $k_p > 0$  as  $S$  approaches infinity.

A possible rationale for a non-zero asymptote might be the intrinsic mechanical structure of paper. Paper fibers are oriented more in the  $x,y$  plane of paper than in the thickness, direction,  $z$ . If a component of lateral travel of light is governed by something like a light-piping effect, independently of scattering, then a fixed  $k_o = 0.25$  mm travel length might be applicable to all commonly encountered papers. This suggests Eq. (16) as a simple, heuristic modification for the MTF of plain papers, shown as the solid line in Fig. 10.

$$k_p = 5.4/S + k_o \quad (16)$$

A drawback of models based on Kubelka–Munk, starting with either Eq. (8) or Eq. (10), is the assumption that the paper samples are of infinite thickness. As demonstrated in Fig. 6, thickness can be of practical significance in determining the MTF of many practical papers. In order to gain some insight into the effect of thickness, sample 20 from Table I was examined by measuring  $k_p$  for a single sheet backed with black,  $R_g = 0$ . Then  $k_p$  was measured for stacks of  $n = 2, 3, 4,$  and  $5$  sheets. The single sheet has a thickness of  $z = 0.11$  mm, and the stacks have thickness  $n \cdot z$ . The thickness can be expressed in terms of scattering distance,  $\ell = S \cdot n \cdot z$ . Figure 11 shows measured values of  $k_p$  for sample #20 versus stack thickness expressed in units of scattering distance,  $\ell$ . The results suggest the sample behaves as an infinitely thick material for a thickness  $\geq 4$  in units of scattering distance,  $L$ . The line shown in Fig. 11 is Eq. (17) with  $k_{p\infty} = 0.990$ , which is the value of  $k_p$  measured for the infinite stack of samples in Table I.

$$k_p = k_{p\infty} \cdot (1 - e^{-\ell}) \quad (17)$$

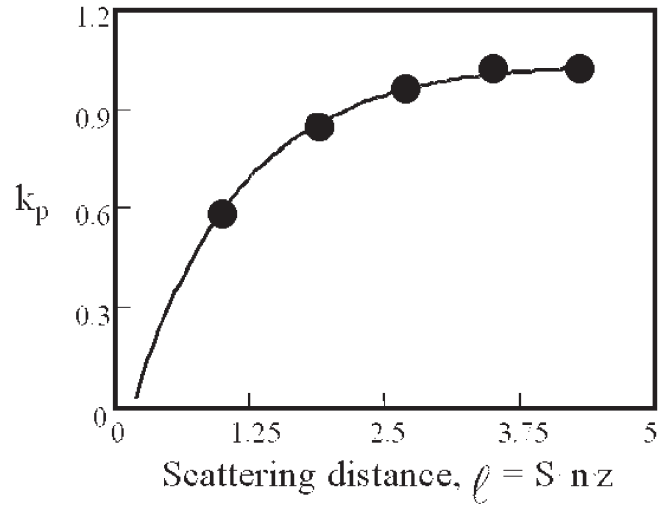


**Figure 11.** Measured value of  $k_p$  (mm) vs thickness,  $\ell$ , in scattering distance for stacks of 1 through 5 sheets of sample 20, Table I. The solid line Eq. (17).

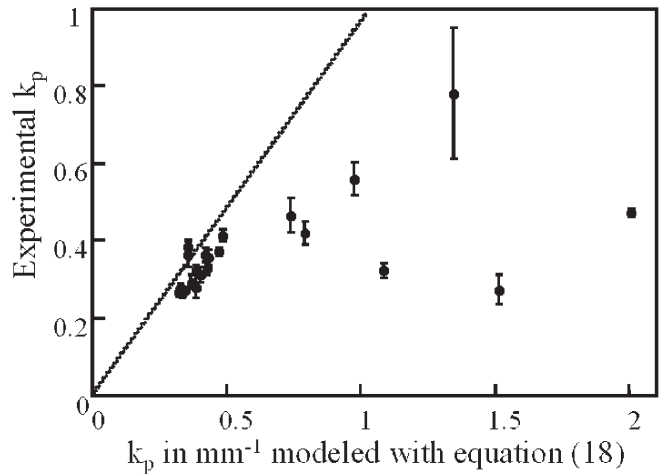


**Figure 12.** Measured values of  $k_p$  versus values of  $k_p$  modeled with Eq. (18) and experimental values of  $S$  and  $z$ . Error bars are  $\pm$  two standard deviations for multiple measurements. The dotted line shows the ideal correlation at slope 1, zero intercept.

If Eq. (17) were generally applicable to all paper samples, then Eq. (18) might be expected to model any sample at any thickness. Using the values of  $z$  and  $S$  in Table I and

$$k_p = \left(\frac{5.4}{S}\right) \cdot (1 - e^{-zS}) + k_o \quad (18)$$

$k_o = 0.25$  mm, values of  $k_p$  were calculated with Eq. (18) and compared with experimentally measured values of  $k_p$  in Table I. Figures 12 and 13 present the results.

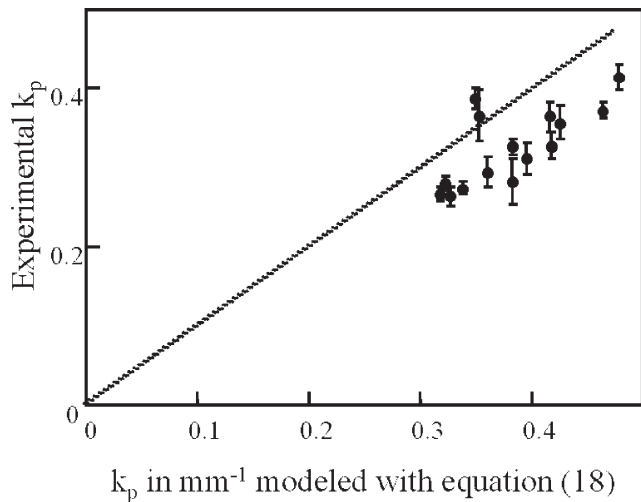


**Figure 13.** Data plot of Fig. 12 confined to values of  $k_p < 0.5$ . The dotted line shows the ideal correlation at slope 1, zero intercept.

### Conclusions

Equation (18) seems to provide an approximate description of the impact of  $S$  and  $z$  on the MTF of paper for values of  $k_p < 0.5$  mm. This is the range for papers most commonly encountered in an office type environment. The correlation between modeled and measured values of  $k_p$  is far from high, but the error bars shown in Figs. 12 and 13 suggest this is not primarily a result of random experimental error. Rather, it appears likely that the Kubelka–Munk parameters  $S$  and  $z$  are not sufficient descriptors of paper MTF, even for papers with the same background ( $R_g = 0$ ) and negligible values of  $K$ . Some additional parameter appears to play a significant role in determining the MTF of printing substrates. This additional parameter may relate to the degree of homogeneity of the substrate. Engeldrum pointed out that any model derived from Kubelka–Munk theory implies the assumption that the scattering coefficient,  $S$ , is homogenous throughout the substrate. Homogeneity in this context means a constant value of  $S$  with respect to depth,  $z$ , and coated papers are a good example

of inhomogeneous substrates. In addition, directional homogeneity is assumed so that  $S$  in the vertical direction is the same as  $S$  in the lateral direction. However, the intrinsic directionality of paper strongly suggests that vertical and lateral scattering distances are probably not the same.

The authors are not aware of an experimental technique for characterizing spatial and directional inhomogeneity in papers. Such an analysis might provide an independent rationale for the observed deviations from the dotted lines in Figs. 12 and 13, and such an investigation might lead to a significant advance in understanding of paper optics.  $\blacktriangle$

**Acknowledgment.** The authors express their appreciation to Hewlett–Packard Corporation for their support of this project.

### References

1. S. Mourad, K. Simon, P. Emmel, and R. D. Hersch, Extending Kubelka–Munk's Theory with lateral light scattering, *NIP17: International Conference on Digital Printing Technologies*, IS&T, Springfield, VA, 2001, p. 469–473.
2. P. Emmel and R. D. Hersch, A unified model for color prediction of halftoned prints, *J. Imaging Sci. Technol.* **44**, 351 (2000).
3. S. Guo and G. Li, Application of Kubelka–munk theory in device-independent color space error diffusion, *Recent Progress in Digital Halftoning II*, IS&T, Springfield, VA, p. 378–382, 1999.
4. S. Gustavson, Color gamut of halftone reproduction, *J. Imaging Sci. Technol.* **41**, 283 (1997).
5. J. S. Arney, C. D. Arney, M. Katsube, and P. G. Engeldrum, An MTF analysis of papers, *J. Imaging Sci. Technol.* **40**, 19 (1996).
6. S. Inoue, N. Tsumura and Y. Miyake, Measuring MTF of paper by sinusoidal test pattern projection, *J. Imaging Sci. Technol.* **41**, 657 (1997).
7. G. Jorgensen, *GATF Research Progress* **47**:1, Pittsburg, PA (1960).
8. P. Oittinen, *Advances in Printing Science and Technology*, vol. 16, W.H. Banks, Ed., Pentech Press, London, UK, 1982, pp. 121–128.
9. P. Oittinen and H. Saarelma, *Paperi Ja Puu Paper & Timber* **75**, 66 (1993).
10. P. G. Engeldrum and B. Pridham, The application of turbid medium theory to paper spread function measurements, *TAGA Proc.* 339 (1995).
11. J. A. C. Yule and W. J. Neilsen, The penetration of light into paper and its effect in halftone reproduction, *TAGA Proc.* 65 (1951).
12. J. A. C. Yule, D. J. Howe and J. H. Altman, The effect of the spread function of paper on halftone reproduction, *TAPPI*, 337 (1967).
13. P.G. Engeldrum, The color between the dots, *J. Imaging Sci. Technol.* **38**, 545 (1994).
14. G.L. Rogers, Optical dot gain: Lateral scattering probabilities, *J. Imaging Sci. Technol.* **43**, 341 (1998).
15. G. Wyszecki and W. S. Stiles, *Color Science: Concepts and Methods*, 2nd ed, John Wiley and Sons, New York, 1982, p. 221.
16. J.S. Arney, E. Pray and K. Ito, Kubelka–Munk theory and the Yule–Nielsen effect on halftones, *J. Imaging Sci. Technol.* **43**, 365 (1998).